RAPID COMMUNICATIONS

PHYSICAL REVIEW A VOLUME 46, NUMBER 10 15 NOVEMBER 1992

Novel cross-roll state in a cylindrical convection cell with thermally conducting sidewalls

K. E. Anderson, M. D. Shattuck, and R. P. Behringer

Department of Physics and Center for Nonlinear and Complex Systems, Duke University, Durham, North Carolina 27706

(Received 11 August 1992)

We describe a new traveling-wave cross-roll state in a water-filled cylindrical convection cell with thermally conducting sidewalls ($\Gamma = D/2d = 4.94$). Just beyond convective onset, four axisymmetric toroidal rolls form. For $\epsilon = (R - R_c)/R_c > 0.15$ this pattern loses stability to either a nonaxisymmetric state with rolls normal to the sidewall, or (by skipping from onset to a value of $0.3 < \epsilon < 1.3$) a pattern consisting of three toroidal rolls with cross rolls in the outermost toroidal roll. The cross rolls are time dependent and typically form modulated traveling waves.

PACS number(s): 47.20.Bp, 47.20.Ky, 47.20.Tg, 47.25.Qv

There has been substantial recent interest in the nonlinear dynamics involved in chaos and pattern selection [1]. An experimental system suitable for studying such phenomena is the Rayleigh-Bénard system. In conventional Rayleigh-Bénard experiments, a horizontal layer of fluid is confined between two highly conducting horizontal plates. The fluid is heated from below, and as the Rayleigh number R, a dimensionless parameter proportional to the vertical temperature gradient, is increased beyond a critical value R_c, convection rolls form within the fluid layer.

Our research examines the convection patterns formed within a small cylindrical container with thermally conducting sidewalls, instead of the more commonly used insulating sidewalls [2]. We have discovered a new convection pattern consisting of three toroidal rolls with cross rolls located in the outermost toroidal roll. These cross rolls are time dependent, typically forming two modulated traveling waves moving in opposite azimuthal directions.

Our apparatus consists of both a cylindrical cell filled with water in a precisely controlled thermal environment and a shadowgraph for visualization of the convective flow. A shadowgraph image shows the horizontal pattern of the flow, with downflow (upflow) regions appearing brighter (darker) in the image. In order to enhance the shadowgraph images, an image obtained in the absence of convection has been digitally subtracted from each image of a convecting state. The cylindrical convection cell has a diameter $D = 4.56$ cm and a height $d = 0.462$ cm, yielding an aspect ratio $\Gamma = D/2d = 4.94$. The vertical thermal diffusion time of the water layer is $\tau_v = d^2/D_T = 147$ sec (where D_T is the thermal diffusivity) and the horizontal diffusion time is $\tau_h = 3.98$ h. The top plate is sapphire, the bottom plate is gold-plated optically flat copper, and the sidewalls are stainless steel with thickness $t = 0.558d$. The sapphire plate is kept at a temperature of 28.2 °C by jets of water from a thermally regulated bath. The resulting flows are independent of the geometry used for the jets. A thin film of nonsoluble silicon grease is used to maintain thermal contact between the horizontal plates and the sidewalls. The thermal conductivity of the stainless-steel sidewalls is 50 times the thermal conductivity of water.

Barkley and Tuckerman [3] used numerical calculations to investigate the effects of sidewall conductivity on axisymmetric convection. They characterized the conductivity of the sidewalls with the parameter $\mu = \pi(\kappa_{\text{wall}}/\kappa_{\text{fluid}})\tanh(\pi t)$, where κ_{fluid} and κ_{wall} are the fluid and wall thermal conductivities [4], and t is the thickness of the sidewall in units of the fluid height d. Barkley and Tuckerman considered containers with aspect ratio $\Gamma = 5$. For $\mu > 60$ and Prandtl numbers $\text{Pr} \geq 5$ they found a bifurcation at $\epsilon = (R - R_c)/R_c = 1.4$ from an axisymmetric, stationary convection pattern of five concentric rolls to an axisymmetric, traveling-wave state. They predicted that this traveling-wave state would propagate from the outer wall inward toward the center of the cell.

Contrary to these predictions our experiments ($\Gamma = 4.94$, $\mu = 148$, and $\text{Pr} = 5.5$) show a stable circular state for $0 < \epsilon < 0.15$, a traveling-wave cross-roll state for $0.18 < \epsilon < 1.5$, and a nonaxisymmetric convection state characterized by the nearly normal intersection of the rolls with the sidewalls for $0 < \epsilon < 2.8$ (the entire range covered by our experiments). The circular roll pattern observed immediately beyond onset has four toroidal rolls with rising fluid in the center of the cell, Fig. 1(a). The cross-roll pattern is generated by making a relatively large jump in ϵ, shifting quickly from $\epsilon < 0.15$ (from below convection or from the circular state) to $0.3 < \epsilon < 1.3$ (the middle of the cross-roll region). The cross-roll state has three axisymmetric toroidal rolls with traveling-wave cross rolls located in the outermost toroidal roll. Typical shadowgraph images of this pattern illustrating the time-dependent behavior of the cross rolls are shown in Figs. 1(c)–1(f) with $0.068\tau_v$ between subsequent images. An example of the nonaxisymmetric state is shown in Fig. 1(b). This state can be generated either by moving beyond the stability limits of the cross-roll state or by making any transition from the pure conduction or circular state other than a jump into the middle of the stable cross-roll range of ϵ. The nonaxisymmetric state includes slowly evolving time-dependent patterns, slowly rotating patterns, and stationary patterns.

There are several important characteristics of the traveling-wave cross-roll state: (1) the traveling-wave frequency is slow, of order $1/\tau_h$; (2) the traveling-wave

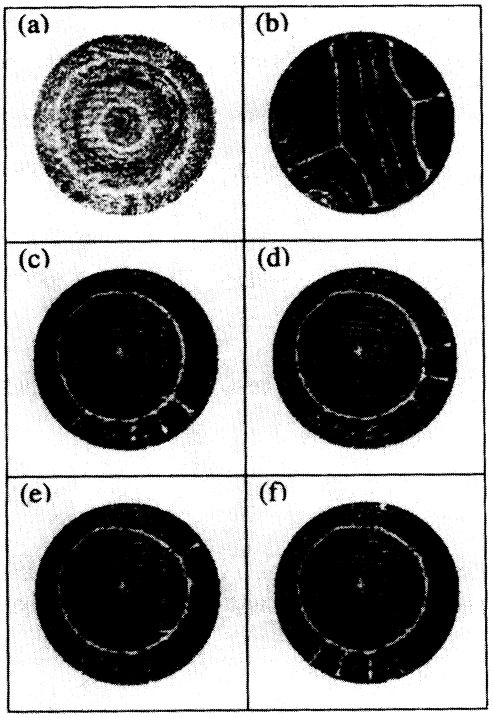

FIG. 1. Shadowgraph images of convection patterns: (a) circular state, $\epsilon=0.03$; (b) nonaxisymmetric state, $\epsilon=2.46$; (c)–(f) cross-roll state, $\epsilon=0.89$. The time between images (c)–(f) is 10 sec$=0.068\tau_v$.

states are usually modulated where the modulation frequency is fast, of order $1/2\tau_v$, and where the modulation corresponds to a starting and stopping (not a reversal) of the convective flow; (3) the phase of the modulation varies over the cross rolls; (4) the wave vector of the cross rolls is approximately twice the fundamental wave vector of the three toroidal rolls in the cell; and (5) for $\epsilon > 1.0$, the cross-roll pattern can become quite complex with multiple traveling-wave frequencies existing simultaneously.

The temporal behavior of the cross-roll state can be seen by plotting the light intensity of the shadowgraph image as a function of angular position and time as shown in Fig. 2. This space-time plot is created by taking a series of digitized shadowgraph images, dividing the annular region of the outermost toroidal roll azimuthally into 256 wedge-shaped bins, and then averaging the intensity of the image within each bin. Figure 2 shows an example of this averaged intensity, translated into a gray scale, as a function of azimuth and time.

In the cross-roll state we have observed modulated, pure, and intermittent traveling waves, where the intermittent pattern consists of an irregular temporal alternation between a pure and a modulated pattern. In Fig. 2 ($\epsilon=0.49$) the cross rolls form two modulated traveling waves propagating in opposite azimuthal directions with a traveling-wave source located at 50° and a sink at 260°. A more complex time dependency is shown in Fig. 3 ($\epsilon=1.42$) with modulated standing waves at 0° and 40°, modulated traveling waves between 60° and 220°, and

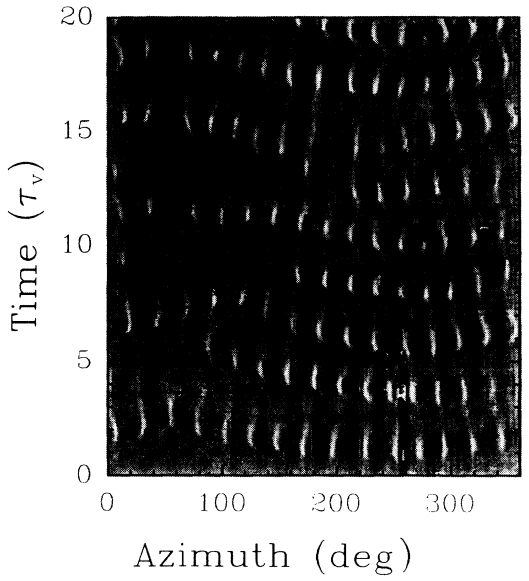

FIG. 2. A space-time plot of the cross rolls showing two modulated traveling waves over $20\tau_v$ (49 min), $\epsilon=0.49$. This plot is created by dividing the cross-roll region of the shadowgraph image (annular region extending from $\frac{2}{3}$ radius to the outer wall) into 256 wedge-shaped bins. The intensity of the digitized shadowgraph image is averaged over each bin and plotted as a function of azimuth and time.

(moving in the opposite azimuthal direction) a mixture of modulated and pure traveling waves between 220° and 340°.

Figure 4 plots (a) the frequency of the modulating wave, f_{mod}, and (b) the traveling-wave frequency, f_{TW}, as a function of ϵ. Both frequencies increase with ϵ, with

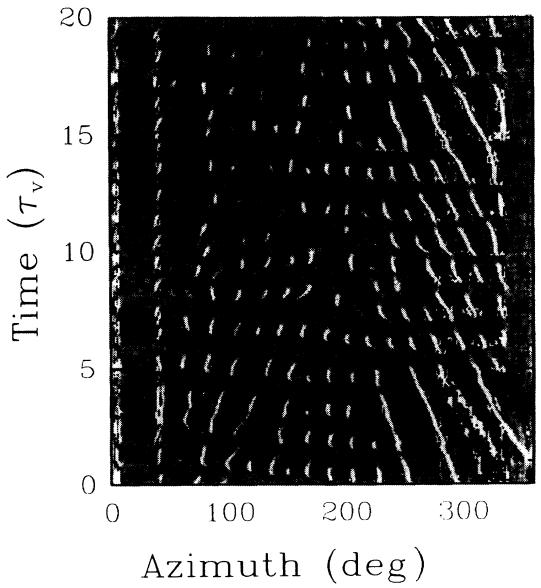

FIG. 3. A space-time plot showing a more complex cross-roll pattern including modulated standing waves, modulated traveling waves, and pure traveling waves, $\epsilon=1.42$.

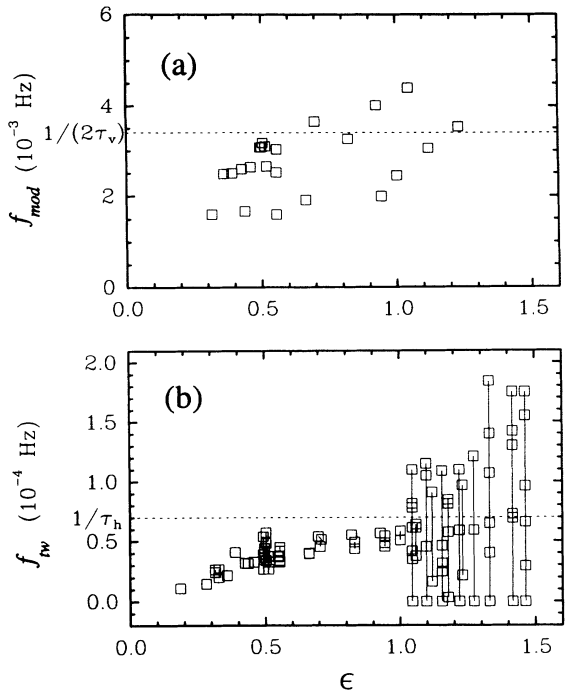

FIG. 4. (a) The modulating wave frequency, f_{mod}, and (b) the traveling-wave frequency, f_{TW}, of the cross rolls as a function of ϵ. The vertical bars connect traveling wave frequencies existing simultaneously within the cell.

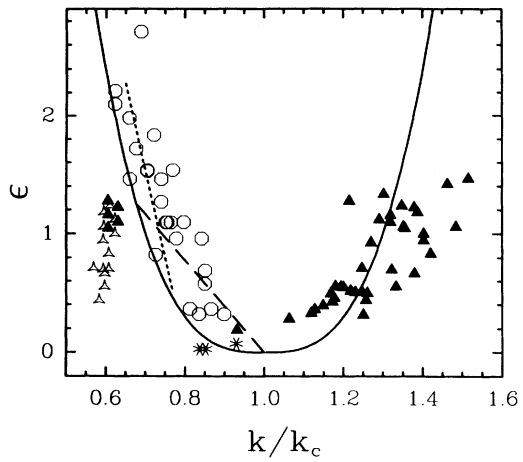

FIG. 5. Wave numbers of the cross rolls (▲), the inner toroidal pattern of the cross-roll state (△), the nonaxisymmetric state (○), and the circular state (*) are shown (normalized by $k_c = 3.117$) along with the zigzag (————) and cross-roll (---) instabilities for Pr=7 [5]. The wave numbers plotted are an average with a typical spread in k/k_c of ± 0.1.

f_{mod} on the same frequency scale as $1/(2\tau_v) = 3.4\times10^{-3}$ Hz and f_{TW} on the same scale as $1/\tau_h = 7\times10^{-5}$ Hz. In Fig. 4(b) multiple traveling-wave frequencies existing simultaneously within the convection cell are connected by vertical bars. For $\epsilon < 1.0$ all traveling-wave frequencies fall within a fairly narrow band about a single curve, but for $\epsilon > 1.0$ a transition occurs, and there is a large spread in traveling-wave frequencies extending to $f_{\mathrm{TW}} = 0$, i.e., to standing waves.

The cross-roll pattern generated is very sensitive to small changes such as physical nonuniformities in the convection cell. By shifting the metal ring which forms the sidewalls of the convection cell slightly off center with respect to the bottom plate heater, thereby creating a nonuniform heat flow through the walls, we can generate convection patterns where the cross rolls are limited to certain azimuthal locations. With the sidewalls shifted even further off center, we could not generate any cross-roll patterns. Even without altering the convection cell, the particular cross-roll pattern formed varies between runs with both pure and modulated traveling waves being observed over the entire Rayleigh number range of the cross-roll state.

Wave numbers for all three states observed in our experiments along with Busse and Clever's calculations (for Pr=7) of the zigzag and cross-roll instabilities in an infinite system of straight rolls [5] are plotted in Fig. 5. The wave numbers of the traveling-wave cross rolls are approximately twice the wave numbers of the toroidal rolls, while the standing-wave cross rolls have a wave number approximately equal to the underlying toroidal rolls. At the onset of the cross-roll state, this doubling of the wave number brings the new cross rolls much closer to the critical wave number than the underlying toroidal rolls. This shifting of the wave number closer to critical is an important result of Busse and Clever's analysis of the cross-roll state and it also distinguishes our stable cross-roll pattern from observations of transient patterns which may appear similar [2].

Analytical work by Jones and Proctor [6] examines the nonlinear interaction between two stable modes having wave numbers in the ratio 1:2. Their calculations, along with the results of Armbruster, Guckenheimer, and Holmes [7] who emphasized a group-theoretic approach, have found that the preferred solutions to this system are traveling-wave states. Standing waves and modulated traveling waves are two other behaviors predicted by their analyses. Although an exact comparison between their results and our experiment is not currently possible, we believe that future work extending their analysis to our system by focusing on the interaction between the cross-roll instability and the original convection rolls may explain the traveling-wave patterns we have observed.

Before concluding we consider possible reasons for the difference between our observations and the predictions of Barkley and Tuckerman. The model of Barkley and Tuckerman assumes infinite isothermal horizontal boundaries. In the experiment, this condition is not strictly met. The relative conductivities κ_{fluid}, κ_{wall}, and the conductivities of the upper sapphire plate, κ_{sap}, and the lower copper plate, κ_{Cu}, fall in the proportion $\kappa_{\mathrm{Cu}}:\kappa_{\mathrm{sap}}:\kappa_{\mathrm{wall}}:\kappa_{\mathrm{fluid}} = 1200:67:50:1$. The comparable conductivity of the sidewalls and the upper sapphire plate will cause some axisymmetric heat flow, an effect which should enhance the stability of the axisymmetric pattern. Barkley and Tuckerman report that for Pr < 5, axisymmetric flow is linearly unstable to an $m=1$ mode. Our experiments, with Pr = 5.5, may be close enough to this boundary that small

perturbations lead to the nonaxisymmetric states. We note that even for complete axisymmetry, there are, for $\Gamma=5$, nonaxisymmetric modes with critical Rayleigh numbers higher than the axisymmetric mode by less than 1% [8].

In summary, convecting water in a small cylindrical container with thermally conducting sidewalls shows complex time-dependent behavior within a cross-roll state. These cross rolls usually form modulated traveling waves with the frequencies of both the traveling and the modulating wave increasing with Rayleigh number. For higher Rayleigh numbers the cross-roll patterns become more complex with multiple traveling-wave frequencies existing simultaneously within the cell, leading to an interesting spatio-temporal complexity. Besides the cross-roll state, a stable axisymmetric convection pattern has been observed at convective onset and a nonaxisymmetric pattern characterized by the normal intersection of the rolls with the sidewalls has been observed over the entire Rayleigh number range studies.

We thank J. Guckenheimer and P. Holmes for helpful discussions on traveling waves in systems with O(2) symmetry. This research was supported by DOE Grant No. DE-FG05-88ER 45371.

[1] P. Berge, Y. Pomeau, and C. Vidal, *Order Within Chaos* (Hermann, Paris, 1984).

[2] C. Meyer, G. Ahlers, and D. S. Cannell, Phys. Rev. Lett. **59**, 1577 (1987); V. Steinberg, G. Ahlers, and D. S. Cannell, Phys. Scr. **32**, 534 (1985); V. Croquette, M. Mory, and F. Schosseler, J. Phys. (Paris) **44**, 293 (1983).

[3] D. Barkley and L. S. Tuckerman, Physica D **37**, 288 (1989); L. S. Tuckerman and D. Barkley, Phys. Rev. Lett. **61**, 408 (1988).

[4] In their papers, Barkley and Tuckerman refer to κ_{wall} and κ_{fluid} as thermal diffusivities. However, in a private communication with these authors, we have established that these should be conductivities, not diffusivities.

[5] F. H. Busse and R. M. Clever, J. Fluid Mech. **91**, 319 (1979).

[6] C. A. Jones and M. R. E. Proctor, Phys. Lett. A **121**, 224 (1987); M. R. E. Proctor and C. A. Jones, J. Fluid Mech. **188**, 301 (1988).

[7] D. Armbruster, J. Guckenheimer and P. Holmes, Physica D **29**, 257 (1988).

[8] G. S. Charlson and R. L. Sani, Int. J. Heat Mass Transfer **14**, 2157 (1971).

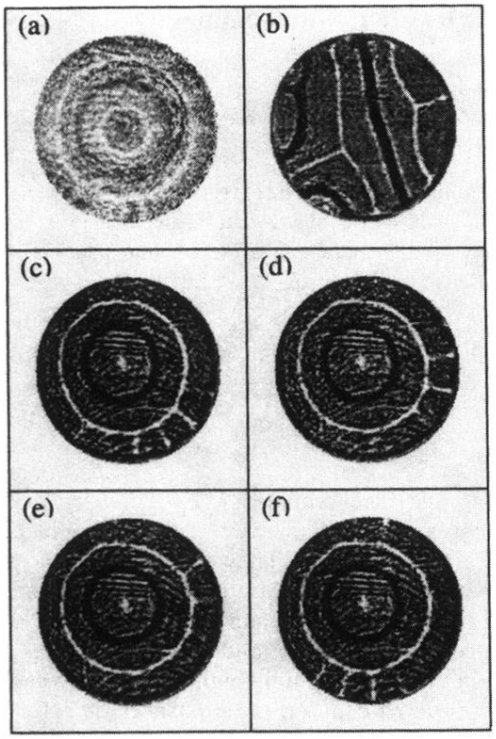

FIG. 1. Shadowgraph images of convection patterns: (a) circular state, $\epsilon=0.03$; (b) nonaxisymmetric state, $\epsilon=2.46$; (c)–(f) cross-roll state, $\epsilon=0.89$. The time between images (c)–(f) is 10 sec$=0.068\tau_v$.

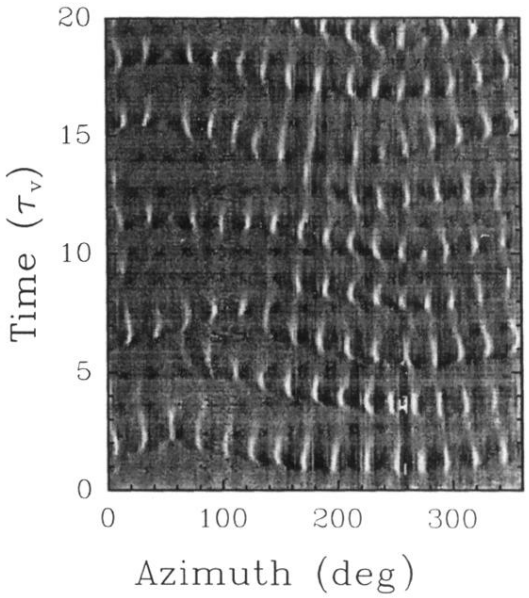

FIG. 2. A space-time plot of the cross rolls showing two modulated traveling waves over $20\tau_v$ (49 min), $\epsilon=0.49$. This plot is created by dividing the cross-roll region of the shadowgraph image (annular region extending from $\frac{2}{3}$ radius to the outer wall) into 256 wedge-shaped bins. The intensity of the digitized shadowgraph image is averaged over each bin and plotted as a function of azimuth and time.

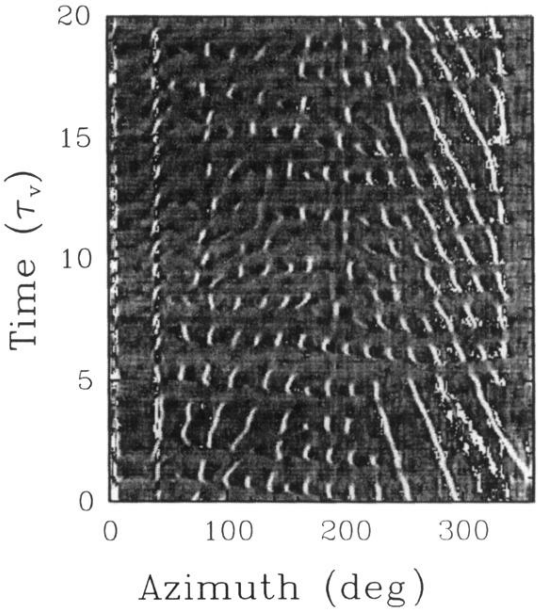

FIG. 3. A space-time plot showing a more complex cross-roll pattern including modulated standing waves, modulated traveling waves, and pure traveling waves, $\epsilon = 1.42$.